2017

Flame propagation of Al/PTFE mechanically activated composites

Michael Huston
Iowa State University

Flame propagation of Al/PTFE mechanically activated composites

by

Michael Huston

A thesis submitted to the graduate faculty

in partial fulfillment of the requirements for the degree of

MASTER OF SCIENCE

Major: Mechanical Engineering

Program of Study Committee:
Travis Sippel, Major Professor
James Michael
Valery Levitas

Iowa State University

Ames, Iowa

2017

TABLE OF CONTENTS

LIST OF FIGURES

Page

NOMENCLATURE

ARM	Arrested, reactively milled
EDS	Energy dispersive X-ray spectroscopy
ESD	Electrostatic discharge
MA	Mechanically activated
PTFE	Polytetrafluoroethylene
SEM	Scanning electron microscopy
TMD	Theoretical maximum density

ACKNOWLEDGMENTS

I would like to thank my major professor Dr. Travis Sippel for giving me a spot in his laboratory and all his mentoring. I would also like to thank my other committee members, Dr. James Michael and Dr. Valery Levitas for being part of my POS committee; I have learned much from their research.

ABSTRACT

The structure of mechanically activated (MA) energetic composites are complex, having at the same time intra-particle reactive length scales as small as sub-micrometer and inter-particle length scales as large as 1 mm. This work investigates the combustion propagation of MA aluminum and polytetrafluoroethylene (PTFE) while varying as-milled particle size, stoichiometry, particle bed density, and confinement to better understand combustion propagation. Propagation rates of MA Al/PTFE are four orders of magnitude slower than similar physically mixed nano-Al/PTFE or micron-Al/PTFE compositions reported elsewhere. Combustion of MA composite beds is found to be macroscopically stable within quartz tubes of >3 mm diameter, though microscopic relay-race combustion is observed in which slow combustion transfers between particles preclude rapid intra-particle combustion. Confined burning rate is increased with reduction of packing density below 55% TMD and burning rate is insensitive to tube end confinement. A maximum burning rate is observed at Al/PTFE ratios of 50/50 wt.%, corresponding to conditions predicted to maximize gas production. Packed beds containing larger (> 75 μm) particles produced 50% faster burning rates than smaller (< 25 μm) particles, and absence of confinement increases burning rate by a factor of ten. Taken together, these results show that the propagation of MA Al/PTFE composites contradicts combustion trends of either purely micrometer-Al/PTFE or nanometer-Al/PTFE packed beds. Findings of this work are consistent with separate results in which laser ignition of single MA Al/PTFE particles results in MA particle microexplosion. It is hypothesized that MA Al/PTFE packed bed combustion is controlled by the rate enhancing effects of microexplosion-induced forward propagation of burning ejecta

within packed beds, leading to maximum burning rates in conditions which promote ejecta propagation. The findings of this work provide important insight into the combustion physics of MA Al/PTFE and similar ‘microexploding’ energetics which must be considered in application.

CHAPTER I

INTRODUCTION

Nanoscale thermites are capable of high energy release and confined burning rates on the order of 100 m/s or higher [1-3]. Several theories have been proposed to explain the high confined burning rates of nanothermites, including forward convection reactive entrainment (i.e. product gas entrainment of reacting particles) [1,4,5], particle ignition enhancement via oxide stress effects (i.e. melt dispersion) [1,4,5], or enhanced oxide shell diffusion [6,7]. While the latter two theories are appropriate for spherical particles of approximately sub-micrometer diameters, it is generally accepted that the interconnected porosity within a nanothermite packed bed enhances forward convection of hot combustion products, which can increase confined burning rate. In a packed nanothermite bed, forward convection directly heats a discrete mixture of fuel/oxidizer particles and ignition is facilitated by high heat localization (i.e. low thermal conductivity) of the packed bed as well as the reduced ignition temperature typical of nanoscale metal (e.g. aluminum) fuel particles [8].

The importance of forward convection and heat localization on nanoscale thermite flame propagation are apparent as density is increased, resulting in reduced gas penetration of the unreacted material and reduced heat localization. In a study of pressed aluminum/molybdenum trioxide (Al/MoO_3) thermite [9,10], it has been observed that for $\mu Al/MoO_3$, increasing density results in a faster burning rate, whereas for nAl/MoO_3, increasing density reduces burning rate. It is hypothesized that the increased burning rate of $\mu Al/MoO_3$ at higher densities is due to conduction enhancement and that the reduced burning rate of nAl/MoO_3 at higher density is due to decreased unreacted bed porosity and

permeability necessary for gas diffusion [10]. Further studies have been conducted measuring the flame propagation velocity of nAl/MoO_3-based [11] and micrometer-Al/CuO-based [12,13] physically mixed thermites in which aluminum particles are thermally treated prior to thermite combustion in order to either damage the oxide skin or artificially grow the oxide skin thickness while imparting residual shell stress upon cooling. These efforts collectively find that damage to oxide skins reduces thermite burning rate and growth of the micrometer-scale oxide shell can enhance thermite burning rate. These findings provide support for the importance of the melt diffusion mechanism [13-15] on thermite combustion. In consideration of thermite packing density, it is suggested that these core-shell aluminum particle ignition dynamics contribute to the increase in thermite burning rate observed at reduced nAl-based thermite packing densities [16].

However, core-shell nanoparticle combustion enhancement mechanisms are not applicable when the thermite is no longer comprised of discrete, spherical fuel and oxidizer particles. Such is the case with mechanically activated (MA) / arrested, reactively milled (ARM) composite energetic materials. Thermite beds produced through MA or ARM contain micrometer-scale particles of irregular or equiaxed shape, each having an internal particle micro/nanostructure of cold welded fuel and oxidizer fragments that develops during the ball milling process. The shapes of fuel and oxidizer interstices within a particle are therefore a function of constituent mechanical properties and milling conditions. As a result of their unique structure, inter-particle length scales are expected to be important to both forward convection and thermal length scales, while intra-particle heterogeneity is expected to control reactivity and heat release rate.

Though more complex in structure than physically mixed thermites, MA composites possess some benefits in comparison to their physically mixed counterparts. The MA or ARM process is a top-down technique [17,18], and as such, is more readily scaled than production of nanoparticles by most other techniques. As nanostructuring is achieved through MA or ARM, feed stocks to this process may be micro-scale rather than nanoscale, achieving lower production cost. Additionally, while nanoscale thermites are sensitive to electrostatic discharge (ESD), friction and impact ignition, MA / ARM thermite composites can be far less sensitive to accidental ignition stimuli [20]. Finally, MA / ARM results in composite particles comprised of both fuel and oxidizer that have full or near-full density; as such both the overall energy content and aging characteristics of MA energetics could be more favorable than nanoparticle mixtures due to their lower oxide passivation layer content [20] and lower particle envelope surface area. Despite these potential benefits, the confined flame propagation of mechanically activated composites remains unstudied.

The purpose of this study is to characterize the confined flame propagation of mechanically activated Al/PTFE composites in channels in order to understand the role that the complex structure of MA composite particle packed beds has on flame propagation. Specifically, the aim of this effort is to investigate the effects of varying as-milled particle size, stoichiometry, packing density, tube diameter, and tube end termination to explore the better understand mechanisms dominating MA composite confined flame propagation. For comparison, similar measurements are conducted on particle packs of nAl/nPTFE and also a μAl/PTFE doped with nAl.

CHAPTER II

EXPERIMENTIAL PROCEDURES

Equilibrium Calculations

Equilibrium combustion calculations were conducted on the anaerobic reaction of aluminum / polytetrafluoroethylene compositions using the Cheetah 8.0 equilibrium software [19]. Atmospheric, constant pressure calculations were conducted for compositions of varying stoichiometry from 10 to 90 wt.% aluminum using the JCZS library and exp6 gas equation of state.

Al/PTFE MA Composite Particle Manufacture

Polytetrafluoroethylene, (PTFE) powders of sizes of ≤12 μm (Sigma-Aldrich), and 80 nm Zonyl (DuPont) were blended with 30 μm aluminum powder (Valimet) at varying stoichiometries from fuel-rich (70/30 wt.%) to fuel-lean (26/74 wt.%). The majority of burning rate measurements were conducted on compositions of 40/60 wt.% Al/PTFE stoichiometry, as these stoichiometries produced the fastest burning rates in compacts of physically mixed thermites investigated by others [3]. Particle average sizes are as-reported by the manufacturer. The sample powders were prepared in 60 mL Cole-Parmer polypropylene containers and then mechanically activated under argon using sixty 3.2 mm (1/8”) and twenty 9.5 mm (3/8”) 440C stainless steel media (McMaster Carr) at a charge ratio of 19:1 in a SPEX 8000M high-energy mill. To prevent on-mill reaction of the energetic, milling was conducted in 1 minute durations followed by 4 minutes of rest time for

a total of 2.5 hours, or 30 minutes of total mill time. Particle composition and phase of similarly prepared materials has been reported elsewhere [20].

Particles were characterized using scanning electron microscopy (SEM) using a FEI Quanta 250 field emission electron microscope. Electron micrographs (Fig. 1) indicate particles are ~10 to 100 μm in size with few large particles (>150 μm) and have thin cross-section. As large particles distributions may adversely affect local flame propagation rates, as-milled Al/PTFE particles were sieved to 25-75 μm prior to use in flame propagation experiments. High magnification electron backscatter compositional images indicate the heterogeneous structure within particles, which contain flakes of aluminum bonded (high intensity / light features) together by layers of PTFE (low intensity / dark features). Aluminum and PTFE compositional features range from roughly 5 to 20 μm. Particle thicknesses measured from similarly manufactured Al/PTFE compositions has been reported elsewhere to be ~12 μm [20].

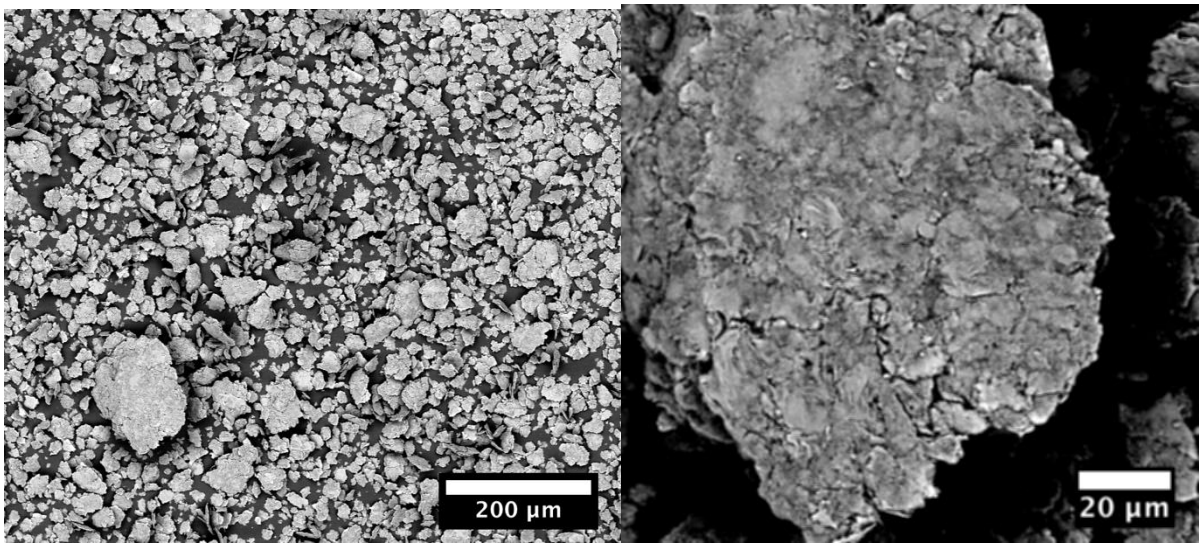

Figure 1. *Left: Low magnification electron microscopy image of Al/PTFE (70/30 wt.%, 30 min MA). Right: High magnification electron microscopy viewgraph of the internal structure of a particle. Images are taken in compositional backscatter mode; dark (low exposure) regions indicate presence of PTFE and bright (high exposure) regions indicate presence of aluminum.*

Combustion Article Preparation

It was observed that polycarbonate tubes char during flame propagation, resulting in visual distortion or obstruction of the flame volume within the tube. As such, in this study, MA composites are packed into 12.7 cm long quartz capillary tubes (Technical Glass Products) with internal diameters of 2, 3, 4, and 5 mm. Quartz was chosen due to its high tensile strength (4.8×10^7 Pa), high melting point, low thermal conductivity, and high light transmissivity (>90% from 230 nm to 1500 nm). Powders were inserted into the tubes and packed to target percent theoretical max densities, TMDs, ranging from 20% to 80%. To achieve uniform densities without gradients, calculated masses of materials were slowly loaded into the capillary tubes while resting on a vibrating table. The tubes were rotated about their axes in the presence of vibrations until compositional densification to the desired packing length (analogous to TMD) was achieved.

In order to explore the effects of forward convection occurring in confined combustion of loose packed powders, the burning rate of near-full TMD pellets was also investigated. Sieved Al/PTFE MA composites were formed into 9.5 mm (3/8”) diameter pellets using a die and 12-ton hydraulic bottle jack press. Packing densities of pellets were measured prior to combustion and were ~96% TMD.

Combustion Experimentation

In order to observe the effects of end confinement on propagation, combustion experiments were conducted with the tube exit (Fig. 2) either open or sealed by epoxy. Composites were ignited using a 7 cm long, 24 AWG (0.51 mm diameter) nichrome wire,

(Consolidated Wire) attached to a Variac. The wires were energized to between 14.4-21.6 VAC to achieve ignition. Propagation data from the first ~2.5 cm of the tube was ignored to prevent skew of data due to the non-uniform density and thermal environment surrounding the ignition wire. Flame propagation was recorded using a Phantom IR300 high speed camera with both a 60 mm (Nikon) lens and a model K2 long distance microscopic lens (Infinity Photo-Optical). Video acquisition rates ranged from 1000 to 6500 Hz. To explore the effects of interstitial gas type (air or inert argon) on burning rate, some combustion articles were drawn down in a vacuum chamber and back-filled with argon and then ignited within an argon-filled glove box.

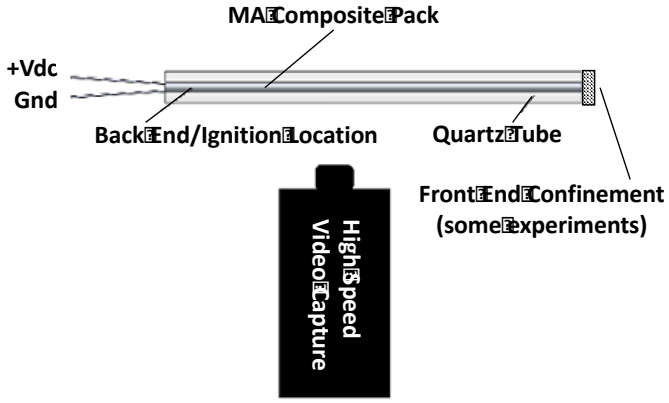

Figure 2. *Confined flame propagation experimental configuration. The tube front end is sealed for some experimental configurations.*

Open tray experiments similar to those of Watson *et al.* [3] were used to assess unconfined burning rate. Polycarbonate material was found to be sufficient for optical observation due to faster open tray burning rates. A 9.525 mm OD, 3.175 mm ID tube was cut lengthwise into a trough. The trough was loaded to tap density with energetic composite which was subsequently ignited under atmospheric conditions via electrically heated nickel chromium wire.

CHAPTER III

RESULTS AND DISCUSSION

Combustion Wave Structure

The combustion progression of MA Al/PTFE compacts within quartz tube confinement is shown in Fig. 3(a), and analysis of flame front position as a function of %TMD (Fig. 3b) shows burning rates to be steady over the range of TMDs explored. As combustion waves neared the ends of the packed tubes, flame front acceleration was observed as the packed bed shifted under the influence of gas pressure; data from these combustion regimes as well as the initial ignition transient were omitted from burning rate analysis.

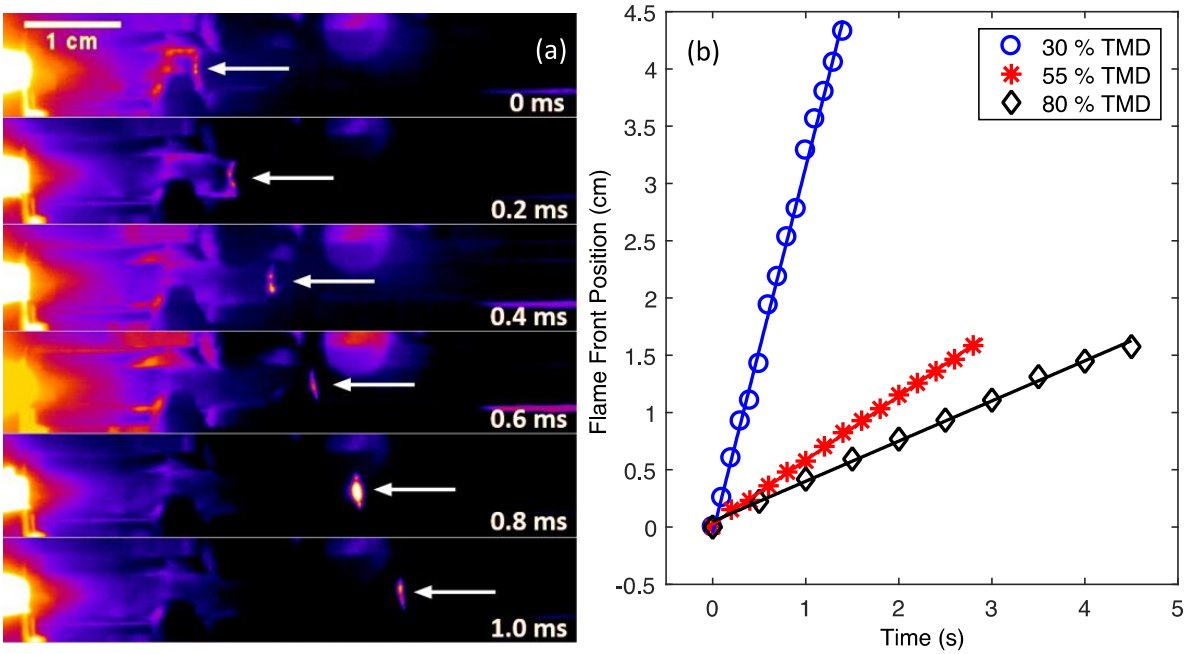

Figure 3. *(a) Flame propagation of a mechanically activated Al/PTFE composition (40/60 wt.%, 75-500 µm, 48% TMD) within a 2mm ID quartz tube. (b) Flame front position as a function of time for the propagation on the left. False color and arrows are used in image sequence to better show flame location.*

The confined combustion propagation of Al/PTFE 40/60 wt.% MA composite particles is observed to occur with the presence of two distinct flame regions (Fig. 4a). A primary flame anchored to the regressing burning surface is observed in addition to a secondary flame anchored to the end of the confinement tube. In order to observe phenomena occurring in the primary flame, microscopic imaging of the propagating combustion wave was conducted (Fig. 4b). High speed video and image sequences of the primary flame propagation indicate presence of a thin ~100 μm to 1 mm thick luminous, condensed phase reaction zone attached to the burning surface. No condensed phase droplets / particulate from the primary flame are observed to entrain in the gaseous combustion product flow. Most notably, image sequences of the combustion of MA Al/PTFE composites, while macroscopically steady, are microscopically an unsteady combustion processes. Analysis of local burning rates within the tube (Fig. 4c) indicates that combustion wave propagation within MA Al/PTFE particle compacts occurs in a 'relay-race' fashion where groups of particles ignite and burn rapidly with slower flame transfer between particles. Similar unsteady 'relay-race' combustion behavior has been observed by Hwang *et al*. in the flame front of both gas/solid reactions (titanium/air) and solid/sold reactions (high energy ball milled Ni/Al) [21]. In consideration of these results, we hypothesize Al/PTFE 'relay-race' combustion is attributed to inter- vs. intra-particle differences in mixing, ignition delay, and heat transfer environment. As such, Al/PTFE relay-race is expected to be most prevalent in particle compacts of low packing fraction (%TMD) and large composite particle size where large differences in inter- and intra-particle spatiotemporal thermal and reactive time scales exist. Confined combustion of MA Al/PTFE composites is admittedly complex due to non-

spherical particulate geometry and differences in length scales within particles and between particles.

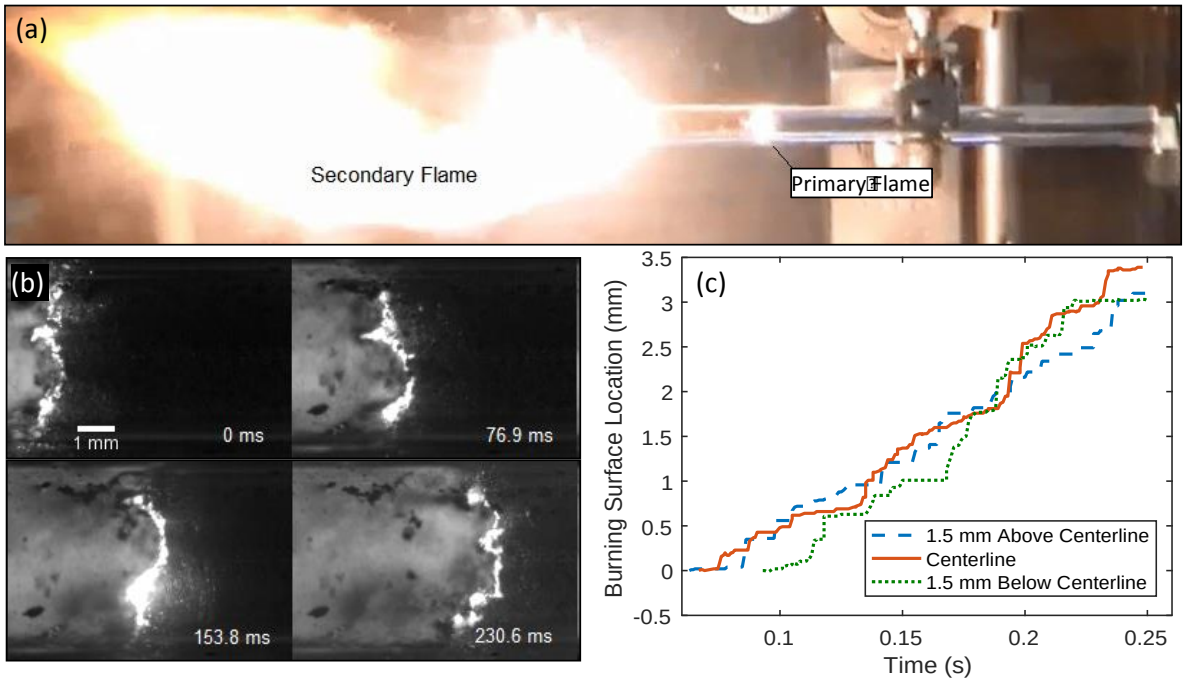

Figure 4. *(a) Still frame image of the confined combustion of Al/PTFE indicating presence of both a surface-attached and secondary combustion flame. (b) Macroscopic progression of a 40/60 wt.% (5 mm ID tube, ~40% TMD). (c) Microscopic progression of the same flame. For these conditions, air mass fraction within the tube is < 0.1 wt.%.*

Further insight into the primary flame can be drawn from equilibrium combustion calculations of the anaerobic reaction of Al/PTFE at 1 atm, as the mass fraction of air present in particle compacts of packing densities explored in this effort are less than ~0.12 wt.%. Shown in Fig. 5(a), the 40/60 wt.% Al/PTFE stoichiometry investigated in this study is predicted to produce both a high adiabatic flame temperature (~3300 K) and high gas production (~15.0 mol/kg reactant). At this composition and flame temperature, combustion products are primarily comprised of solid carbon, gaseous aluminum subfluorides (AlF, AlF_2), and gaseous aluminum trifluoride (AlF_3) (Fig. 5(b)). At more fuel-rich

stoichiometries, additional aluminum fuel availability results in higher gas production due to preferential formation of gaseous aluminum subfluorides rather than aluminum trifluoride and at leaner conditions, higher resulting flame temperatures are supported by preferential formation of lower energy aluminum trifluorides. Within the observable flame (Fig. 5(a)), carbon formed from PTFE decomposition occurs in sub-micrometer smoke particles and upon exiting the quartz tube, produces a diffusion flame in combustion with atmospheric air. The amount of energy released in complete combustion of the secondary flame (3940 kJ/kg Al/PTFE) is similar to the amount of energy released in the primary flame. For compositions containing ~40 to ~60 wt.% Al, the adiabatic flame temperature remains 2740 K, and is insensitive to Al/PTFE ratio due to Al vaporization enthalpy requirements. At more fuel-rich stoichiometries (> 60 wt.% Al), liquid aluminum equilibrium combustion products become prevalent.

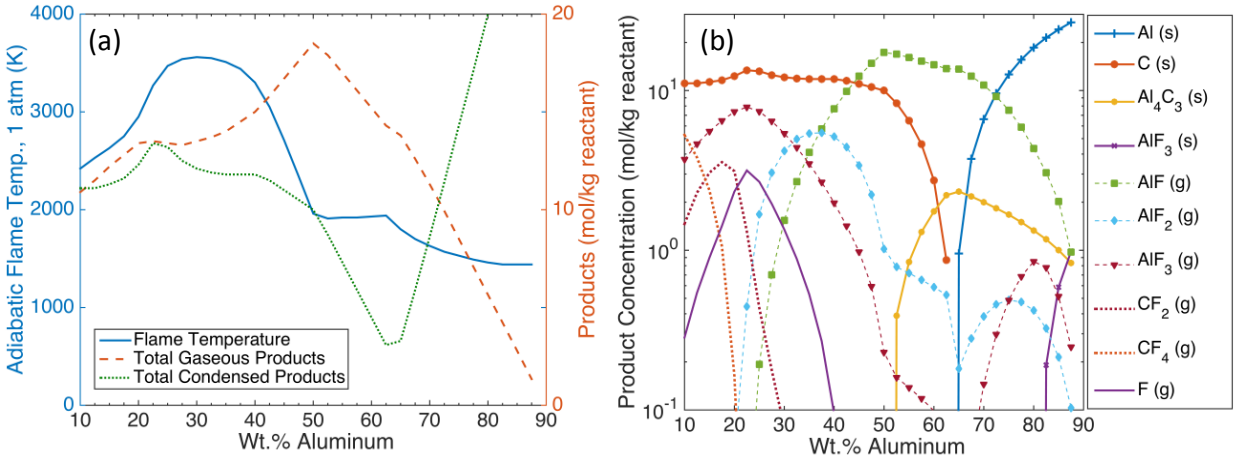

Figure 5. *(a) Adiabatic flame temperature and equilibrium gas production of anaerobic, atmospheric pressure combustion of Al/PTFE as a function of composition. (b) Equilibrium combustion products of the same.*

Effect of Internal Tube Diameter

Although microscopic propagation is unsteady, steady macroscopic propagation rates of ~2.4 cm/s is achieved without thermal quenching within quartz tubes having inner diameters from 3 to 5 mm (Fig. 6(a)). The propagation rate was found to fluctuate widely within diameters of 2 mm, as is evident from the higher standard deviation of rate measurement data and flame quenching was also frequently observed within 2 mm ID tubes. In addition to the effects of thermal loss, high burning rate variability and quenching in small tube diameters are also expected to be attributed to nonuniformities in tube packing expected as tube diameter approaches sieved particle distribution sizes of 25-75 µm. In comparison to confined burning rates of discrete particle mixtures of 50 nm nAl/nPTFE (~800 m/s) and 2 µm Al/nPTFE (~300 m/s) with similar stoichiometry [3], the measured burning rates of mechanically activated Al/PTFE composites are roughly four orders of magnitude slower.

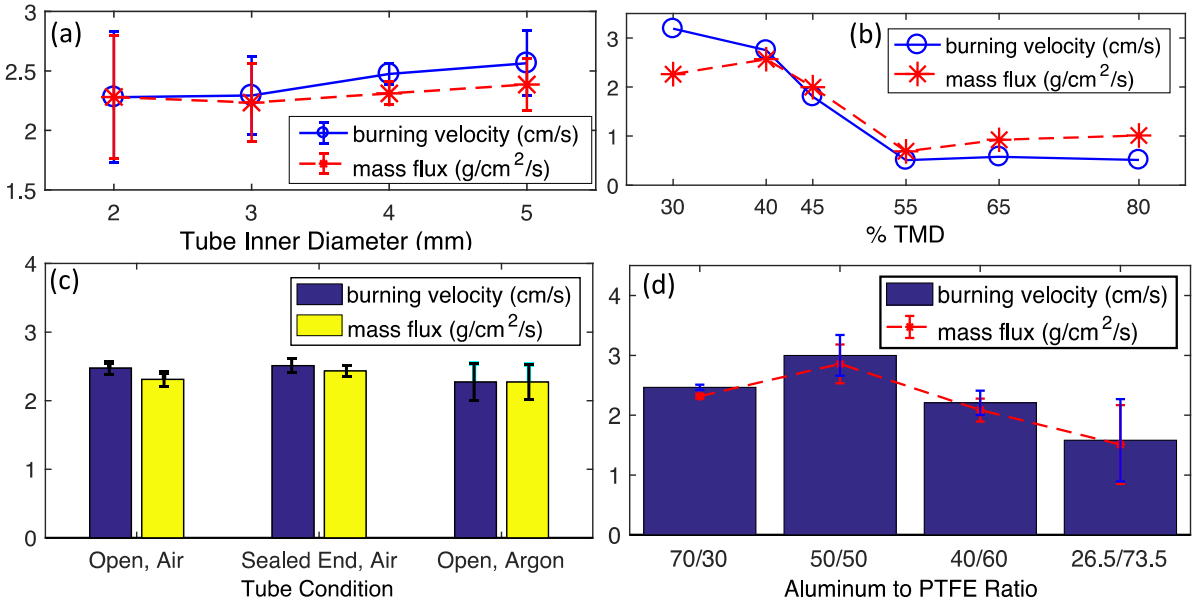

Figure 6. *(a) Combustion wave propagation rate as a function of quartz tube diameter (~40% TMD). (b) Combustion wave propagation rate as a function of % TMD within 5 mm ID tube. (c) Combustion wave propagation rate as a function of tube end confinement condition and interstitial gas environment (4 mm ID tube, ~40% TMD). (d) Combustion wave propagation rate for Al/PTFE MA composites (3 mm ID, ~40% TMD) with varying*

stoichiometry. All compositions are Al/PTFE (40/60 wt.%, 30 min MA, sieved 25 – 75 µm) unless indicated otherwise. Error bars indicate one standard deviation of experiments.

Effect of Variation of Packing Density

Measurement of burning rate as a function of %TMD (Fig. 6(b)) indicates that burning rate is relatively insensitive to density above 55% TMD, and at lower densities, burning rate increases from ~0.5 cm/s (55% TMD) to ~3.3 cm/s (30% TMD). Burning rate measurements were additionally conducted on 9.5 mm diameter pellets of MA Al/PTFE pressed to ~96% TMD (Fig. 7) in which burning rates were measured to be 0.90 to 1.1 cm/s similar to the burning rates of 55% to 80% TMD confined propagation rates.

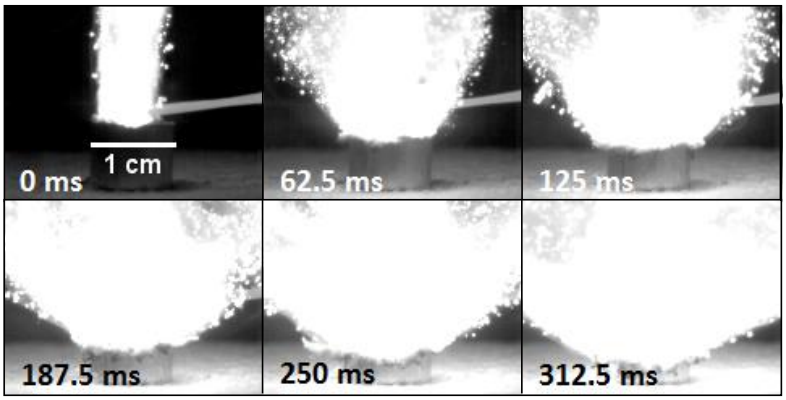

Figure 7. *Flame propagation of a 9.53 mm diameter, near 100% TMD pellet of MA Al/PTFE 40/60 wt.% composite.*

The measured propagation rates of near full density pellets (Fig. 7) reinforces the finding of packing density does not significantly affect MA Al/PTFE burning rates at densities greater than 55% TMD. Measured flame propagation rates within unconfined beds reinforces findings that in compacts with < 55% TMD, reduction in %TMD increases confined burning rate. Despite having much slower burning rates than physically mixed thermites of nAl/nPTFE [3], the general trend of increased MA Al/PTFE burning rate as a

function of % TMD is similar to the trend describing nAl-based thermites observed by Pantoya *et al*. [10], indicating that unlike micrometer-scale particulate thermites, intra-particle conduction is poor due to high numbers of Al/PTFE interfaces, and increased packing density does not improve forward thermal conduction into the unreacted particle bed. It is hypothesized that increased burning rates at lower packing density are a result of forward heating caused by ejection of hot particle fragments from reacting Al/PTFE particles. Briefly, observation of laser ignited single MA Al/PTFE particles by Rubio *et al.* [22] has demonstrated that under high irradiation flux conditions, MA Al/PTFE particles ignite and rupture due to gas-producing intra-particle reactions, producing dispersions of high velocity condensed phase reacting mixtures. Observed shattering of reacting composite particles, which occurs at sufficiently high laser flux, is hypothesized to result from internal particle pressurization due to (1) PTFE decomposition product evolution and (2) propagation of flames along intra-particle fuel/oxidizer interfaces to the interior of composite particles. As such, it is believed that faster burning rates of MA Al/PTFE at lower packing densities are also a result of enhanced forward dispersion of hot combustion products that most effectively enhance burning rates in low density compacts.

It is expected that at packing densities above 55%, pressure drop of the particle bed is significantly high to impede forward convection. The effect of particle shape and resulting packing density on pressure drop is admittedly complex. It has been shown that variation of packing density of a bed of monodisperse spherical particles results in different particle packing structures of hexagonal close, offset cubic, or simple cubic arrangement which correspondingly result in variations in packed bed pressure drop [23]. Additionally, separate experimental results suggest that irregular particle shape (low sphericity) and broader particle

size distribution which are both typical of Al/PTFE MA composite energetics [20] can more than double the pressure drop of a packed bed, and increased surface roughness has been found to also adversely affect pressure drop [23]. At high packing densities, compaction may also result in particle deformation convection inhibition due to sealing of the tube. Further investigations of the effects of particle shape and packing density on pressure drop, though outside the scope of the current effort, should be conducted.

Tube End Confinement and Gas Environment Condition

Forward convection of gaseous combustion products has been proposed to control the burning rate of nanoscale aluminum-based thermites [16]. In order to explore the effects of forward convection on MA Al/PTFE burning rate, experiments were conducted in which the exit of the tube is sealed to prevent forward convection of gaseous combustion products through the unreacted particle bed. Additionally, packed tubes were evacuated, backfilled with argon gas, and burned in an argon gas environment in order to assess the effect of interstitial gas on burning rate. Figure 6(c) shows that burning rates of open ended tubes burned in air, argon, and sealed tubes burned in air all have burning rates of ~2.3 to 2.5 cm/s. These results suggest that forward convection of gaseous combustion products is not significant due to a substantial pressure drop in the tightly packed capillary due to the aforementioned effects of particle geometry on pressure drop. Burning rates in open ended tubes filled with both air and argon were ~2.5 and ~2.3 cm/s, respectively, indicating that at 21 vol.% O_2 atmospheric conditions, the presence of air has little effect on the combustion propagation of MA Al/PTFE composites. This is expected, as unlike nAl-based thermites where metal particle interfaces are predominantly exposed to environmental gas, intraparticle

reactive interfaces within MA Al/PTFE are more tightly packed and environmental gas presence at reactive interfaces is less prevalent. Experiments conducted on combustion of iodate, cupric oxide, and iron oxide based nAl thermites by Farley *et al*. [23] in either a 4 vol.% or 93 vol.% atmospheric pressure O_2/Ar environment suggest that for slow burning rate thermites in which combustion is diffusion controlled, the presence of excess oxygen has a more significant effect on flame speed enhancement (~30 % increase for 80 nm Al + 15 μm $Ca(IO_3)_2$ and ~100 % increase for 80 nm Al + 40 μm Fe_2O_3). The 8% decrease in mechanically activated Al/PTFE burning rate that occurs with removal of ~21 vol.% O_2 indicates that diffusion effects in MA Al/PTFE packed beds, though not particularly strong, are also not insignificant. Kinetic enhancement may also contribute to enhanced rates with increased oxygen content, as the presence of O_2 during Al/PTFE reactions has been shown to alter reaction pathways and shorten reaction times through activation of kinetic pathways involving initial fluorocarbon fragment oxidation [24,25].

Flame propagation experiments were conducted on unconfined MA Al/PTFE particle beds within an open burn tray configuration similar to that of Watson *et al.* [3] were conducted, where the free surface at the top of the particle compact is a free air interface, providing an unconstrained combustion propagation surface. Figure 8 shows the forward progression of a reacting flame in an unconfined bed. Flame structure is very different from that of confined configurations: rather than a thin primary flame attached to the reacting bed and a secondary flame, a single flame over the surface of the reacting material is observed. Measured burning rates of MA Al/PTFE in unconfined bed configurations were found to be 0.29 m/s, approximately ten times faster than confined rates. These measured burning rates are roughly 3 and 10 times slow than micrometer-scale and nanometer-scale Al/PTFE

particulate thermites of the same composition that were explored by Watson *et al.* [3]. The effect of confinement on flame propagation of MA composite Al/PTFE is opposite the effect observed in combustion of nAl/nPTFE thermites, where confinement has been observed to increase thermite burning rate [3].

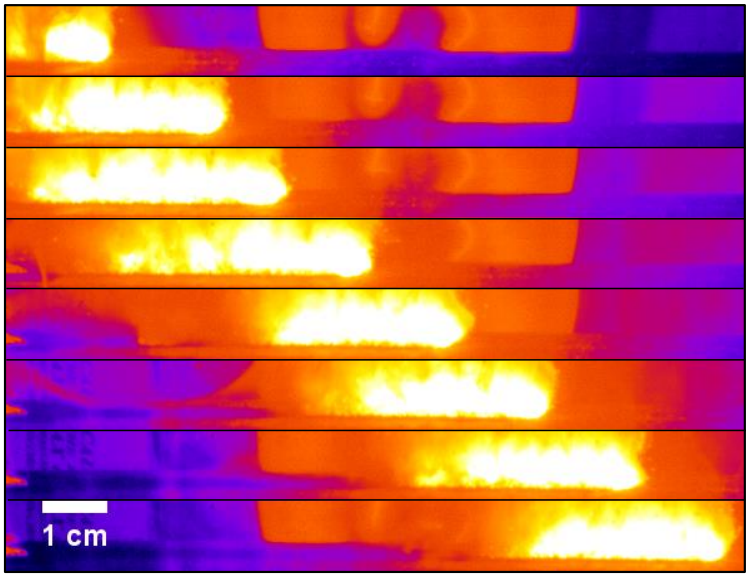

Figure 8. *Unconfined combustion propagation of Al/PTFE 40/60 wt. % MA composite in a 3 mm wide trench. Images in the sequence indicate 50 ms time intervals and are shown in false color.*

In supplemental video, forward moving burning particle fragments can be seen being ejected ahead of the flame front in support of the experimental results of Rubio *et al*., which show MA Al/PTFE particle ignition can result in dispersion of hot, reacting particle fragments [22]. In tube confinement, MA Al/PTFE particles are inhibited from forward ejection resulting in burning rates orders of magnitude slower than nAl or µAl based Al/PTFE [3] particulate mixtures. Conversely, the free surface of an open bed enables more efficient burning rate enhancement by microexplosions ejecta, resulting in open tray burning rates similar to µAl/PTFE [3].

Effect of Stoichiometry

Figure 6(d) shows the effects of varying particle stoichiometry. While an Al/PTFE ratio of 25/75 wt.% has the highest adiabatic flame temperature and is near stoichiometric for production of AlF_3, the fastest burning rates ~3 cm/s were produced from 50/50 wt.% Al/PTFE compositions which correspond roughly to the highest adiabatic gas production through more preferential formation of aluminum monofluoride (Fig. 5a). In discrete particle Al/PTFE thermites of both micrometer- and nanometer- scale, Watson *et al* found that peak confined burning rate occurs at a similar 50/50 wt.% Al/PTFE ratio [3,15]. In spherical particulate compacts, it is hypothesized that peak burning rate occurs at the highest gas production stoichiometry due to enhanced forward convective heating of combustion products. However, in confined beds of MA Al/PTFE, gas production is expected to enhance burning rate through enhancement of microexplosion ejecta velocity, as MA Al/PTFE burning rates are not dependent upon tube end confinement condition (Fig. 6c).

Effect of As-Milled Particle Size

It has been observed in laser ignition of MA Al/PTFE particles that the degree of particle microexplosion increases with increasing particle size as a result of greater intra-particle confinement during internal gas production [22]. In order to explore these effects on the confined propagation of MA Al/PTFE composites, confined tube combustion experiments were conducted on MA Al/PTFE sieved to different size fractions (Fig. 9). It was observed that in increasing the MA Al/PTFE particle size from < 25 μm to > 500 μm, compact burning rate is increased from ~2 to 3.5 cm/s, suggesting larger MA particle size can increase confined burning rates through forward propagation of microexplosion ejecta. In

confined configurations, particularly, microexplosions should be enhanced by presence of larger particles, as compacts of larger particles having similar packing density should contain fewer, but larger porosity within which microexplosions can lead to combustion enhancement. In addition to burning rate enhancement due to more frequent microexplosion, increasing MA Al/PTFE particle size could increase burning rate through increase in condensed phase conduction path lengths within individual particles.

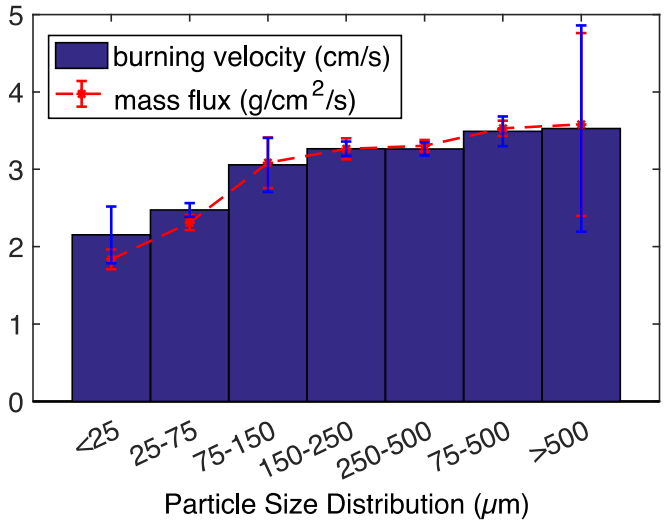

Figure 9. *Combustion velocity of Al/PTFE (40/60 wt.%) packed beds as a function of post-MA sieved particle size (4 mm ID tube, 40% TMD). Error bars indicate one standard deviation of 3 experiments.*

CHAPTER IV

CONCLUSIONS & FUTURE WORK

This work provides important insight into the combustion propagation of granular compacts of mechanically activated Al/PTFE particles through control of confinement, compact packing density, stoichiometry, and interstitial gas composition. Sieved compacts were found to propagate planarly without significant wall quenching effects in tube diameters of > 3 mm (a tube to particle diameter ratio of ~50 to 100). Below 3 mm, quenching was prevalent as the tube diameter approached sieved particle size.

Packed beds of MA Al/PTFE composites possess physical characteristics unique to both nanometer- and micrometer-scale physically mixed thermites, in that while overall particle/particle and particle/interstitial gas length scales are micrometer-scale, but intra-particle reactive length scales are nanoscale. Attributing to their unique physical structure, the combustion propagation of MA Al/PTFE packed beds is unique. The combustion of MA Al/PTFE is observed to be a macroscopically steady but locally/microscopically unsteady process due to the microexplosion phenomena observed elsewhere in study of MA Al/PTFE ignition and significant differences in inter- and intra- particle length scales. As a consequence of their unique structure, confined propagation rates of MA Al/PTFE composites are ~1-3 cm/s, roughly four orders of magnitude slower than the propagation of rates of micron- and nano-Al/PTFE physically mixed particulate beds investigated by others. Maximum burning rates of MA Al/PTFE packed beds are found to occur at 50/50 wt.% Al/PTFE compositions, which produce the highest quantity of gaseous equilibrium combustion products. Additionally, while the burning rate of MA Al/PTFE beds is found to

increase with reduction of packing density below 55% TMD, forward convection does not globally affect the propagation rate, as tube end confinement has no effect on burning rate. A ~50% increase in burning rate is observed in increasing MA composite particle size from < 25 μm to > 500 μm and burning rates of packed beds in open trays absent of wall confinement are found to be ~10 times faster (0.29 m/s) than confined burning rates.

Taken together, these results show the distinct difference in MA Al/PTFE propagation behavior in comparison to either purely micron-Al/PTFE or purely nano-Al/PTFE combustion propagation trends. The combustion of micron-Al/PTFE packed beds is hypothesized to be controlled by forward conduction, whereas combustion of nano-Al/PTFE packed beds is hypothesized to be controlled by unique nAl ignition phenomena and forward convection. The substantial differences in MA Al/PTFE packed bed flame propagation between either nano- or micron- thermites of the same is believed to be a result of MA Al/PTFE particle ignition microexplosion processes and the rate-enhancing forward travel of burning ejecta.

Future efforts in the area of MA composite bed propagation are suggested to explore (1) the effects of the degree of mechanical activation on propagation and (2) enhancement of microexplosion characteristics (e.g. reduction of ignition delay and enhancement of intra-particle pressurization and burning rate). The degree of MA treatment is used to control nanostructure within composite particles and is expected to have a significant effect on intra-particle burning rates. Further inclusion/doping of MA particles with energetic materials having low ignition temperature and/or high gas production may further enhance combustion rate. The coating of particles may additionally enhance flame spread and subsequently reduce

particle ignition delays. It may also be possible to engineer high temperature stability coatings to enhance particle microexplosions through pressure vessel-like effects.

REFERENCES

[1] Levitas VI, Asay BW, Son SF, Pantoya ML. Melt dispersion mechanism for fast reaction of nanothermites. Appl Phys Lett 2006;89:071909.

[2] Densmore JM, Sullivan KT, Gash AE, Kuntz JD. Expansion Behavior and Temperature Mapping of Thermites in Burn Tubes as a Function of Fill Length. Propell Explos Pyrot 2014;39:416–22. doi:10.1002/prep.201400024.

[3] Watson KW, Pantoya ML, Levitas VI. Fast reactions with nano- and micrometer aluminum: A study on oxidation versus fluorination. Combust Flame 2008;155:619–34.

[4] Dikici B, Dean SW, Pantoya ML, Levitas VI, Jouet RJ. Influence of Aluminum Passivation on the Reaction Mechanism: Flame Propagation Studies. Energy & Fuels 2009;23:4231–5. doi:10.1021/ef801116x.

[5] Levitas VI, Pantoya ML, Dean S. Melt dispersion mechanism for fast reaction of aluminum nano- and micron-scale particles: Flame propagation and SEM studies. Combust Flame 2013. doi:10.1016/j.combustflame.2013.11.021.

[6] Park KH, Lee DW, Rai A, Mukherjee D, Zachariah MR. Size-resolved kinetic measurements of aluminum nanoparticle oxidation with single particle mass spectrometry. J Phys Chem B 2005;109:7290–9.

[7] Rai A, Park KH, Zhou L, Zachariah MR. Understanding the mechanism of aluminium nanoparticle oxidation. Combustion Theory and Modelling 2006;10:843–59.

[8] Yetter RA, Risha GA, Son SF. Metal particle combustion and nanotechnology. Proceedings of the Combustion Institute 2009;32:1819–38. doi:10.1016/j.proci.2008.08.013.

[9] Pantoya ML, Granier JJ. Combustion behavior of highly energetic thermites: Nano versus micron composites. Propell Explos Pyrot 2005;30:53–62.

[10] Pantoya ML, Levitas VI, Granier JJ, Henderson JB. Effect of Bulk Density on Reaction Propagation in Nanothermites and Micron Thermites. Journal of Propulsion and Power 2009;25:465–70. doi:10.2514/1.36436.

[11] Gesner J, Pantoya ML, Levitas VI. Effect of oxide shell growth on nano-aluminum thermite propagation rates. Combust Flame 2012;159:3448–53. doi:10.1016/j.combustflame.2012.06.002.

[12] McCollum J, Pantoya ML, Tamura N. Improving aluminum particle reactivity by

annealing and quenching treatments: Synchrotron X-ray diffraction analysis of strain. Acta Mater 2016;103:495–501. doi:10.1016/j.actamat.2015.10.025.

[13] Levitas VI, Pantoya ML, Dikici B. Melt dispersion versus diffusive oxidation mechanism for aluminum nanoparticles: Critical experiments and controlling parameters. Appl Phys Lett 2008;92:011921.

[14] Levitas VI, Asay BW, Son SF, Pantoya ML. Mechanochemical mechanism for fast reaction of metastable intermolecular composites based on dispersion of liquid metal. J Appl Phys 2007;101:83524.

[15] Levitas VI, Pantoya ML, Watson KW. Melt-dispersion mechanism for fast reaction of aluminum particles: Extension for micron scale particles and fluorination. Appl Phys Lett 2008;92:201917.

[16] Levitas VI. Mechanochemical mechanism for reaction of aluminium nano- and micrometre-scale particles. Phil Trans R Soc Lond A 2013;371:20120215–5. doi:10.1098/rsta.2012.0215.

[17] Dreizin EL. Metal-based reactive nanomaterials. Prog Energ Combust 2009;35:141–67. doi:10.1016/j.pecs.2008.09.001.

[18] Suryanarayana C. Mechanical alloying and milling. Progress in Materials Science 2001;46:1–184.

[19] Bastea S, Fried LE, Glaesemann KR, Howard WM, Kuo IW, Souers, P. C., et al. Cheetah 8.0 User Manual. 8 ed. Livermore, CA: Lawrence Livermore National Laboratory Energetic Materials Center; 2015.

[20] Sippel TR, Son SF, Groven LJ. Aluminum agglomeration reduction in a composite propellant using tailored Al/PTFE particles. Combust Flame 2014;161:311–21. doi:10.1016/j.combustflame.2013.08.009.

[21] Hwang S, Mukasyan AS, Varma A. Mechanisms of combustion wave propagation in heterogeneous reaction systems. Combust Flame 1998;115:354–63. doi:10.1016/S0010-2180(98)00016-9.

[22] Rubio MA, Gunduz IE, Groven LJ, Sippel TR, Han CW, Unocic RR, et al. Microexplosions and ignition dynamics in engineered aluminum/polymer fuel particles. Combust Flame 2017;176:162–71. doi:10.1016/j.combustflame.2016.10.008.

[23] Farley CW, Pantoya ML, Levitas VI. A mechanistic perspective of atmospheric oxygen sensitivity on composite energetic material reactions. Combust Flame 2014;161:1131–4. doi:10.1016/j.combustflame.2013.10.018.

[24] Losada M, Chaudhuri S. Finite size effects on aluminum/Teflon reaction channels under combustive environment: A Rice–Ramsperger–Kassel–Marcus and transition

state theory study of fluorination. J Chem Phys 2010;133.

[25] Losada M, Chaudhuri S. Theoretical Study of Elementary Steps in the Reactions between Aluminum and Teflon Fragments under Combustive Environments. J Phys Chem A 2009;113:5933–41.

APPENDIX A

CALCULATION DEFINITIONS

Calculation of Stoichiometric Fuel/Oxidizer Mass Ratio (balanced for C and AlF_3)

The stoichiometric composition is calculated based on production of AlF_3, the lowest energy form of aluminum fluoride.

$$4(Al) + 3(C_2F_4) \xrightarrow{yields} 4(AlF_3) + 6(C), \tag{1}$$

$$\frac{m_{Fuel}}{m_{Fuel}+m_{Oxidizer}} = \frac{N_{Al}MW_{Al}}{N_{Al}MW_{Al}+N_{PTFE}MW_{PTFE}} = 26.5\ wt.\%, \tag{2}$$

where reactant molecular weights are MW_{Al} – 26.982 g/mol, $MW_{C_2F_4}$ – 100.015 g/mol.

Calculation of Composition Percent Theoretical Maximum Density

Percent TMD of a packed granular bed within a confined tube is calculated as the percentage of the theoretical maximum or true density of a fully dense compact, where the theoretical maximum density is calculated as

$$TMD = \frac{m_{Al-PTFE}}{V_{Al-PTFE}} = \frac{m_{Al}+m_{PTFE}}{\frac{m_{Al}}{\rho_{Al}}+\frac{m_{PTFE}}{\rho_{PTFE}}}. \tag{3}$$

The density of the packed bed is calculated as

$$\rho_{Bed} = \frac{m_{Al}+m_{PTFE}}{\frac{\pi}{4}D_{Tube}{}^2 L_{Tube}}. \tag{4}$$

The percent theoretical maximum density of the compact is calculated as

$$\%TMD = \frac{\rho_{Bed}}{TMD}. \tag{5}$$

APPENDIX B

HIGH ENERGY BALL MILLING PROCEDURE

Procedure For:	High energy mechanical activation (small scale, SPEX milling)
Date Created:	01/29/2013
Location:	1056 Black Engineering

Notes:

Potential hazards and Mitigation:

- Ignition of confined reactive – Use of PPE (gloves, safety glasses, cotton clothing, etc.) and clearing of T-Cell during mixing
- Handling of pyrophoric solids/reactives – two people aware of and/or present to ongoing activities

Limitations of procedure: No more than 5 gram total energetic are to be manufactured at once.

Section 1 – PPE to be used during handling of milled energetic

☐ 1. Cotton/organic fiber clothing/lab coat (no nylon/synthetic fiber)

☐ 2. Leather gauntlet gloves

☐ 3. Safety glasses

☐ 4. Face shield

☐ 5. Long pants

☐ 6. Close-toed shoes

Section 2 – Materials/equipment required

☐ 7. SPEX 8000 mixer/miller – mill needs to be controllable from separate room such that room is never occupied while mill is on.

☐ 8. Mill cycle timer

☐ 9. Outlet Power Timer

☐ 10. Cooling fan

☐ 11. 30 mL HDPE plastic bottle

☐ 12. stainless steel milling media

☐ 13. vacuum oven with argon purge

☐ 14. Fuel: _____

☐ 15. Oxidizer: _____

Section 3 – Mixer Preparation and start procedure

☐ 16. NOTE: at least one other person must be aware of ongoing activities for Section 3 of these procedures.

☐ 17. Put on PPE: safety glasses, nitrile gloves, cotton lab coat/clothing, respirator (if required for powders used)

☐ 18. Fill container with milling media: generally 20 large media (SS, 9.5 mm diameter, 3.48 g/media) and 60 small media (SS, 3.175 mm diameter, 0.44 g/media). Weigh media prior to use.

☐ 19. Fill container with **___ gram total powder (no more than 5 gram may be milled at a time with this procedure)**. For this test, will use _____ wt.% fuel and _____ wt.% oxidizer.

☐ 20. Fill container with argon gas by purging with 3 purge cycles in the vacuum oven (at room temperature).

☐ 21. Seal container lid and reinforce with electrical tape

☐ 22. Take off respirator (if respirator was used)

☐ 23. Place container on SPEX mill

☐ 24. Turn on cooling fan—set fan speed to high.

☐ 25. Exit milling room and close doors

☐ 26. Place appropriate warning sign over door handle indicating researchers not enter and also supplying your name, phone number, and the date.

☐ 27. Plug in the cycle timer into the outlet power timer

☐ 28. Set cycle timer to ___1__ minute on, __4___ minute off = ___5___ min/cycle

☐ 29. Set outlet power timer for ___150_____ min. (____30____ cycles x ____5__ min/cycle).

☐ 30. Start mill (start both cycle timer and outlet power timer simultaneously)

Section 4 – Procedure to pull milled material sample/check material

☐ 31. NOTE: at least one additional person must be present for Section 4 of these procedures.

☐ 32. Once the power outlet timer ends, the SPEX mill will automatically turn off. Ensure this by unplugging the cycle time from the outlet power timer. Allow fan to continue to run.

☐ 33. Wait 10 minutes prior to entering milling room.

☐ 34. While waiting, put on PPE (cotton attire, safety glasses, leather gauntlet gloves, face shield).

☐ 35. After 10 minutes, enter milling room

☐ 36. Turn off fan

☐ 37. Transfer milling container to portable glove box

☐ 38. Place hexanes in the glove box (in case material is found to be pyrophoric)

☐ 39. Seal the portable glove box.

☐ 40. Remove PPE (except for safety glasses) and put on medium weight cotton knit gloves (for heat and melt protection when using rubber glove box gloves.

☐ 41. Purge portable glove box with argon until >0.3 vol.% O_2 is detected.

☐ 42. Open milling container and extract small (~5-10 mg) sample of energetic.

☐ 43. Seal milling container

☐ 44. Transport powder sample out of glove box using antechamber box.

☐ 45. Test powder sample sensitivity (pyrophoricity, flame, impact, friction, etc.). Repeat as desired.

☐ 46. If material is found to be pyrophoric:

a. Ensure milling container is tightly sealed and no lose powder is inside the glove box
b. Stopping argon flow and open the glove box
c. Place in glove box a metal sieve pan containing ~1 cm of hexane.
d. Re-establish atmosphere (as described in Step 9), remove from milling container powder to be air passivated and removed. Place powder in hexane-filled metal pan, taking care to submerge all powder and evenly spread powder over the pan surface, eliminating any lose powder piles.

e. If storing some of the non-air stable material, re-seal milling container tightly. Otherwise, leave empty, material-free container open.

f. Stop glove box purge flow and remove hexane and powder-filled metal tin. Place tin under vent fan and behind a blast shield in gas gun room. Label material appropriately. Leave material to dry for 24 hours, allowing powder to air passivate while being cooled by hexane evaporation.

☐ 47. Prior to stopping argon flow and opening glove box, ensure milling container is tightly sealed and no lose powder is inside the glove box.

☐ 48. Put back on PPE listed Step 4 prior to opening glove box and removing milling container.

☐ 49. Reinforce container seal with electrical tape.

☐ 50. If addition milling is to be completed, continue to wear PPE and return to Section 3, Step 5.

☐ 51. If milling container is to be stored, mark container with appropriate warnings and store sealed in an appropriate locked metal storage cabinet for mixed energetics.

Section 5 – Storage, Handling, and Disposal of Materials

☐ 52. Storage: All materials produced in this process need to be stored in an appropriate locked energetic material storage cabinet.

☐ 53. Handling: When handling this material, the following PPE must be used: safety glasses, leather gloves, and cotton clothing.

☐ 54. Disposal: Use approved REM procedures or contact supervisor

Section 6 – Emergency Procedures

☐ 55. Unintentional ignition of material resulting in bodily injury: If minor injury is sustained from the incident (e.g., minor burns), treat with appropriate first aid and contact a supervisor (Travis Sippel, 765-426-2366; Jim Dautremont). If major injury is sustained, immediately call 911 and then contact a supervisor.

☐ 56. Unintentional ignition of material resulting in uncontrolled fire: Ensure that fire is extinguished using appropriate fire extinguisher and then contact a supervisor. **Important:** trying to extinguish a burning metal fire with a class a, b, or c fire extinguisher will worsen flame. Fire must be extinguished with class d extinguisher or met-l-x metal firefighting agent. Met-LX powder. If fire cannot be safely extinguished, immediately pull a fire alarm, evacuate

the building, call 911, and then contact a supervisor. If a fire is sufficiently controlled (e.g., unintentional ignition of paper on a burn plate), let the fire self-extinguish, and then contact a supervisor.

☐ 57. Unforeseen injury: If minor injury is sustained from the incident (e.g., cuts, minor burns, etc.), treat with appropriate first aid and immediately contact a supervisor. If major injury is sustained, call 911 and then contact a supervisor.

The following list of researchers have been authorized to use this procedure:

Name	**Training Date**
Michael Huston	2015/5/20

Instructor: _____Travis Sippel_____

Signature: _____

APPENDIX C

PACKING AND IGNITION OF CONFINED BURN TUBE APPARATUS

Procedure For: Packing and Ignition of Confined Burn Tube Apparatus

Date Created/Created By: 7/17/2014 Michael Huston

Location: Black Eng. Bld. Rm: 1056, Nanoscale Energetics Lab

Number of people required for procedure: 2

Section 0 – Potential Hazards and Mitigation

☐ 1. Ignition of confined reactive mitigation: steel frag box, blast panels and face shield

☐ 2. Know location and us of

- Met-LX metal firefighting agent (under optics table).
- ABC fire extinguisher. (Do not use on metal fires).

Section 1 – PPE to be used during handling of milled energetic

☐ 3. Cotton/organic fiber clothing/lab coat (no nylon/synthetic fiber)

☐ 4. Nitrile gloves.

☐ 5. Safety glasses.

☐ 6. Face shield.

☐ 7. Long pants.

☐ 8. Close-toed shoes.

☐ 9. Plexiglass UL Level 3 shields.

Section 2 – Materials/equipment required

☐ 10. Premixed energetic in a 50 mL HDPE bottle.

☐ 11. Calipers

☐ 12. Ring clamps.

☐ 13. Micro funnel.

☐ 14. Plexiglas/quartz burn tube.

☐ 15. Vibration plate.

☐ 16. Nickel Chromium wire.

☐ 17. Kimwipe plug.

☐ 18. Electronic scale.

☐ 19. Phantom camera.

Section 3 – Preparation and start procedure

☐ 20. Put on PPE.

☐ 21. Measure internal diameter and length of Plexiglas/quartz tube.

☐ 22. Plug one end of Plexiglas/quartz tube with Kimwipe plug.

☐ 23. Weigh mass of energetic material containment bottle.

☐ 24. Turn vibration plate on to just over 50%.

☐ 25. Slowly pour energetic material through micro funnel while holding tube on the vibration table, gently tap down when needed.

☐ 26. Weigh mass of energetic material containment bottle.

☐ 27. Repeat steps 4-8 until 40% TMD is reached.

☐ 28. Secure open end of tube and flip over on the vibration table until the composite material shifts

☐ 29. Maintaining the seal on both ends of the tube and hold on the table lengthwise until the composite material flows – this ensures an even % TMD without density gradients

☐ 30. Place Plexiglas/quartz tube in ring clamps.

☐ 31. Ensure the power supply is off, leads are disconnected and shunted at the power supply.

☐ 32. Form a 7 cm length nickel chromium wire into a pinched V shape with coiled ends.

☐ 33. Place wire into tube and clamp with gator clips then remove Kimwipe plug.

☐ 34. Enclose with Plexiglas shields.

☐ 35. Set up Phantom camera.

Section 4 – Procedure to ignite energetic material

☐ 36. Open Phantom software and adjust settings as desired.

☐ 37. Leave room, sound buzzer for 10 seconds and active warning lights. Make sure on one is in the test room at this time.

☐ 38. Unshunt electrical plug and attach to power source.

☐ 39. Ignite the material.

☐ 40. If ignition is successful, unplug and reshunt electrical plug. Wait one minute before turning off warning lights and reenter the test room to take the setup down.

☐ 41. Crop and save Phantom data. Do not unplug or power off camera until data is saved or it will be lost.

Section 5 – Procedure for the event of a misfire

☐ 42. If the material fails to ignite or appears to have only partially fire, leave the warning lights flashing, unplug the ignition source and turn on the buzzer.

☐ 43. Do not enter the test room for 30 minutes.

☐ 44. Turn off buzzer but leave the warning lights flashing.

☐ 45. Put on PPE: See section 1.

☐ 46. Enter the room and visually inspect the burn tube apparatus for any signs of possible ignitions such as smoke or light.

☐ 47. If visual or physical inspection show signs of possible ignition, leave the test room, turn the buzzer on and wait another 30 minutes.

☐ 48. If inspection shows no signs of possible ignition, disconnect the nickel chromium wire and inspect the energetic material for damage.

☐ 49. If the material shows signs of damage, tap out the damaged portion behind the Plexiglas shield and refill with new material.

☐ 50. Attach a new nickel chromium wire and reset all equipment.

☐ 51. Repeat section 4 procedure.

Section 6 – Emergency Procedures

☐ 52. Unintentional ignition of material resulting in bodily injury: If minor injury is sustained from the incident (e.g., minor burns), treat with appropriate first aid and contact a supervisor (Travis Sippel, 765-426-2366; Jim Dautremont, ((515) 294-6590). If major injury is sustained, immediately call 911 and then contact a supervisor. Contact information for Mary Greeley Hospital: 1111 Duff Ave, Ames, IA 50010, Phone: (515) 239-2011.

☐ 53. Unintentional ignition of material resulting in uncontrolled fire: Ensure that fire is extinguished using appropriate fire extinguisher and then contact a supervisor. **Important:** trying to extinguish a burning metal fire with a class a, b, or c fire extinguisher will worsen flame. Fire must be extinguished with class d extinguisher or met-l-x metal firefighting agent. Met-l-x powder is located in a 5-gallon bucket under optics table in 1056 black. Pour/throw met-l-x firefighting agent on fire to extinguish. Let fire sit until cool for one hour before stirring/touching fire products. Stirring may reignite fire. If fire begins to burn

again, pour additional met-l-x on fire to quench and suffocate fire. If fire cannot be safely extinguished, immediately pull a fire alarm, evacuate the building, call 911, and then contact a supervisor. If a fire is sufficiently controlled (e.g., unintentional ignition of paper on a burn plate), let the fire self-extinguish, and then contact a supervisor.

☐ 54. Unforeseen injury: If minor injury is sustained from the incident (e.g., cuts, minor burns, etc.), treat with appropriate first aid and immediately contact a supervisor. If major injury is sustained, call 911 and then contact a supervisor.

Approved By: _____ 2015/7/17

Travis Sippel Date

The following list of researchers have been authorized to use this procedure:

Name	**Training Date**
Michael Huston	2015/7/17